fire

MDPI

Article

The Effects of Fire Severity on Vegetation Structural Complexity Assessed Using SAR Data Are Modulated by Plant Community Types in Mediterranean Fire-Prone Ecosystems

Laura Jimeno-Llorente [1], Elena Marcos [1,*] and José Manuel Fernández-Guisuraga [1,2]

[1] Departamento de Biodiversidad y Gestión Ambiental, Facultad de Ciencias Biológicas y Ambientales, Universidad de León, 24071 León, Spain; ljimel00@estudiantes.unileon.es (L.J.-L.); jofeg@unileon.es (J.M.F.-G.)
[2] Centro de Investigação e de Tecnologias Agroambientais e Biológicas, Universidade de Trás-os-Montes e Alto Douro, 5000-801 Vila Real, Portugal
* Correspondence: elena.marcos@unileon.es

Abstract: Vegetation structural complexity (VSC) plays an essential role in the functioning and the stability of fire-prone Mediterranean ecosystems. However, we currently lack knowledge about the effects of increasing fire severity on the VSC spatial variability, as modulated by the plant community type in complex post-fire landscapes. Accordingly, this study explored, for the first time, the effect of fire severity on the VSC of different Mediterranean plant communities one year after fire by leveraging field inventory and Sentinel-1 C-band synthetic aperture radar (SAR) data. The field-evaluated VSC retrieved in post-fire scenarios from Sentinel-1 γ^0 VV and VH backscatter data featured high fit (R^2 = 0.878) and low predictive error (RMSE = 0.112). Wall-to-wall VSC estimates showed that plant community types strongly modulated the VSC response to increasing fire severity, with this response strongly linked to the regenerative strategies of the dominant species in the community. Moderate and high fire severities had a strong impact, one year after fire, on the VSC of broom shrublands and Scots pine forests, dominated by facultative and obligate seeder species, respectively. In contrast, the fire-induced impacts on VSC were not significantly different between low and moderate fire-severity scenarios in communities dominated by resprouter species, i.e., heathlands and Pyrenean oak forests.

Keywords: C-band; fire impact; Mediterranean Basin; resprouters; seeders; Sentinel-1; Sentinel-2; synthetic aperture radar; vegetation structure

Citation: Jimeno-Llorente, L.; Marcos, E.; Fernández-Guisuraga, J.M. The Effects of Fire Severity on Vegetation Structural Complexity Assessed Using SAR Data Are Modulated by Plant Community Types in Mediterranean Fire-Prone Ecosystems. *Fire* **2023**, *6*, 450. https://doi.org/10.3390/fire6120450

Academic Editors: Fuquan Zhang, Ting Yun, António Bento-Gonçalves and Luis A. Ruiz

Received: 23 October 2023
Revised: 14 November 2023
Accepted: 17 November 2023
Published: 24 November 2023

1. Introduction

Mediterranean ecosystems of southern European countries have been prone to fire for millennia because of the seasonal climate [1], which promotes high fuel accumulation rates in mild winters, and favorable conditions for fire ignition and spread in hot, dry summers [2]. Accordingly, wildfires in this region are deemed an evolutionary force shaping species adaptation and landscape diversity and thus an integral part of ecosystem dynamics [3,4]. However, wildfires have been traditionally considered hazards with negative connotations and sometimes socioeconomic disasters because of the associated damage to human assets and even loss of lives [5]. In addition, wildfires may entail large ecological effects on plant communities [6–8], soil physicochemical and biological properties [9–12]), hydrogeological processes [13,14], and wildlife [15,16] in the Mediterranean Basin. This has led to special concerns since Mediterranean terrestrial ecosystems in this region hold a large number of endemisms [17] and are considered a biodiversity hotspot [18].

In southern European countries, as in other Mediterranean regions worldwide, there has been evidence of abrupt changes in the natural fire regime that have led to extreme wildfire events in recent years [1,5,19], such as in Portugal in 2017, in Greece in 2018 and 2023, or in Spain in 2021 and 2022. This new scenario has been attributed to global change drivers, such as rural land abandonment and climate change [11,20–22]. Also, forestry

policies based on reforestation, mainly of flammable pine trees, have promoted landscapes dominated by pyrophytic vegetation prone to extreme fire behavior [23].

In the Mediterranean ecosystems of southern European countries, natural fire regimes have contributed to favoring species fire-adaptive traits that facilitate the resilience of fire-prone ecosystems to fire [24,25]. However, altered disturbance regimes as a consequence of global change drivers, including an increase in extensive high-severity wildfires, may entail unprecedented consequences for the stability, resilience, and functioning of Mediterranean fire-prone ecosystems [25–27]. Severe wildfires, defined as those causing a major ecological change with respect to the pre-fire scenario [28], operationally measured based on the biomass consumption by the wildfire [29], may significantly alter land surface energy budgets, leading to a forcing on the feedbacks governing the regional-to-global climate [30]. Besides high aboveground biomass consumption, severe wildfires may hinder seedling recruitment during the early post-fire stages and cause failure in the resprouting response [31,32], thus potentially modifying the structure and composition of post-fire plant communities [33]. Severe wildfires may also induce significant impacts in soil organic matter pools, as well as the volatilization, immobilization, or transformation of soil nutrients [9,10,34,35]. Altogether, these well-documented impacts may lead to a decrease in ecosystem functions and services provided by fire-prone ecosystems, as well as diminished resilience and shifts towards alternative stable ecosystem states [36]. Nevertheless, the fire-induced impact on vegetation structural complexity (VSC) has not been as well studied, particularly in Mediterranean ecosystems with varying fire severity degrees, despite the essential role it plays in absorbing the disturbance before shifting to alternative ecosystem steady states, i.e., promoting ecosystem resilience to fire [37–39]. VSC is also implicated in ecosystem stability and functioning in fire-prone landscapes [4,40]. First, the diversity of plant functional traits is highly related to the vegetation physical arrangement in the vertical profile [41,42]. Second, greater structural diversity is related to increased plant primary production and soil nutrient availability [42,43]. Third, VSC is closely connected to the ecological niche and species habitat [44], including that for avian and insect species in multiple ecosystems [45,46]. Therefore, it is essential to improve knowledge on the effects of fire severity on VSC for providing (i) integrated insights on the maintenance of ecosystem functions and services in post-fire landscapes [4,47] and (ii) scientific-technical advice in the context of ecosystem restoration [48]. Although field inventories are highly reliable for assessing VSC on local scales [49–51], this approach is not feasible for making wall-to-wall assessments in large burned areas and making inferences with sufficient spatial representativeness and exhaustiveness [52]. This is particularly relevant since whether or not severe wildfires modify vegetation structure variability may depend on plant community types and the pre-fire vegetation structure and thus on fire history [25,53]. For instance, Foster et al. [54] found that variability in the vegetation structure was reduced only by severe burns in woodlands rather than forests and shrublands because of the legacy effects of previous wildfires in southeastern Australia. In mixed conifer forests in the Sierra Nevada of California, Lydersen et al. [55] reported that areas burned at high fire severity had a significantly lower tree density for all species types and size classes. Conversely, different post-fire recovery dynamics among forests dominated by seeder or resprouter species resulted in varying magnitudes of fire effects on the evenness of the cover distribution between strata in conifer and mixed forests in northwestern Italy [56]. The loss of canopy cover by strata for a given fire intensity differed for each forest type within the Yosemite National Park [57]. Accordingly, the development of wall-to-wall products is of utmost importance to capture the high variability in VSC behavior with respect to the fire severity inherent to each plant community type in complex burned landscapes.

In this context, remote sensing data from earth observation satellite (EOS) missions enable wall-to-wall post-fire assessments to be performed in a cost-effective manner over extensive areas [48,58]. Conventionally, passive optical remote sensing data, such as spectral indices [59,60], image fractions gathered from pixel unmixing models [48,61], or biophysical variables retrieved through radiative transfer models [36], have been used as

resilience indicators depicting the recovery of vegetation top-op-canopy traits. Conversely, active remote sensors, such as synthetic aperture radar (SAR) and light detection and ranging (LiDAR), can efficiently estimate the vertical structure attributes of vegetation canopies [52,62] because they are sensitive to scattering elements in the canopy in terms of quantity and distribution [63]. LiDAR data are often constrained in post-fire assessments because of the low availability of on-demand airborne acquisitions [44].

Despite the unlimited availability of open-access SAR data acquired by sensors on-board EOSs, such as Sentinel-1 (C-band sensor), and the physical sense of SAR backscatter in burned areas [64], previous studies have seldom considered the use of SAR data to assess VSC in burned landscapes [65], nor the link between the observed responses in VSC as modulated by the fire severity and plant community type in complex post-fire landscapes, although remarkable interactions between those two factors can be expected not only because of different fire resistance patterns between plant communities, but also because of different vegetation responses (e.g., seeders vs. resprouters) in the short term after the fire [36,66]. Accordingly, this study explored, for the first time, the effect of fire severity on the VSC of different Mediterranean plant communities one year after the fire by leveraging field inventory and Sentinel-1 C-band SAR backscatter data as a means of obtaining representative VSC estimates on the entire wildfire scale. Specifically, we selected as case study site a large burned landscape in the western Mediterranean Basin comprising typical Mediterranean shrubland and forest communities.

2. Materials and Methods

2.1. Study Site

The study site is was located in the Sierra the Cabrera mountain range (northwestern Spain, western Mediterranean Basin; Figure 1). The site has a rough topography, dominated by prominent crests with steep slopes and narrow valleys. The altitude ranges between 836 and 1938 m above sea level. The climate is typically Mediterranean, depicting hot and dry summers and cold and wet winters [65], with annual mean temperature and annual mean precipitation ranging between 5 and 15 °C and 600 and 1500 mm, respectively, for a 50-year period [1]. The wildfire affected, between 21 August and 27 August 2017, around 9940 ha of shrublands and forest dominated by the facultative seeders Genista hystrix Lange (gorse community) and *Genista florida* L. (broom community), the obligate seeder *Pinus sylvestris* L. (Scots pine), as well as *Erica australis* L. (Spanish heath) and *Quercus pyrenaica* Willd. (Pyrenean oak) resprouters. The dominant plant communities in the study site were spatially explicitly mapped using a maximum likelihood algorithm [67] applied to a pre-fire Sentinel-2 multispectral instrument (MSI) Level-2A image, with an overall accuracy of 91% and balanced users' and producers' accuracy [68]. Extreme meteorological conditions were recorded during the preceding months of the wildfire, translating into severe fire weather during fire spread [65].

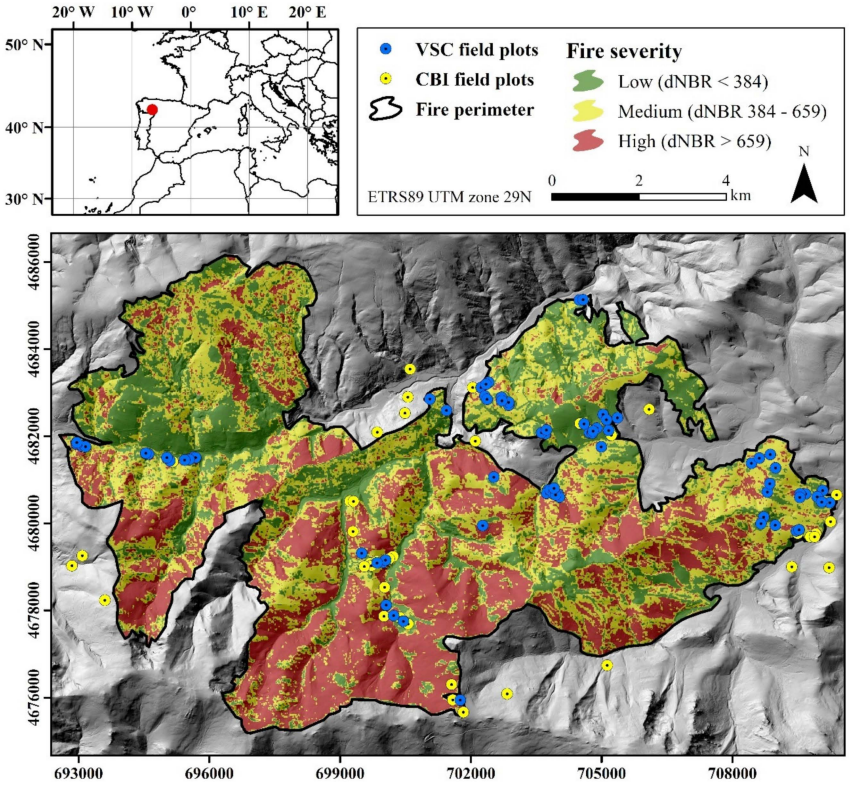

Figure 1. Location of the Sierra the Cabrera wildfire in the western Mediterranean Basin, fire severity classification layer according to the difference of the Normalized Burn Ratio (dNBR) thresholds, and location of the Composite Burn Index (CBI) and vertical structural complexity (VSC) field plots. The background image corresponds to a hillshade product computed from a digital elevation model (DEM) acquired from the Spanish National Plan for Aerial Orthophotography (PNOA).

2.2. Field Inventories

One month after the fire (September 2017), 72 field plots of 20 m × 20 m (19 unburned control plots) were randomly established in relatively homogeneous areas regarding fire effects within the wildfire scar (Figure 1) to conduct an initial assessment of fire severity. The size of the plots is coincident with the spatial resolution of Sentinel-2 MSI data used to obtain wall-to-wall fire severity estimates. The Composite Burn Index (CBI) [69] was measured in each plot. The CBI integrates the magnitude of the combined fire effects in all existing ecosystem strata per plot, including the (i) soil substrate, (ii) herbs, shrubs and trees less than 1 m tall, and (iii) shrubs and trees 1–4 m tall in the understory, and (iv) intermediate trees 4–20 m tall, and (v) large trees taller than 20 m in the overstory. The height strata were slightly modified with respect to the original CBI protocol to better adapt to the characteristics of the plant communities of the study site. In the soil substrate stratum, we recorded char attributes and the percent consumption of fine fuel. For the understory layer (i.e., strata less than 1 m tall and strata 1–4 m tall), we recorded the percent of foliage consumed. In the overstory layer (i.e., intermediate trees 4–20 m tall and large trees taller than 20 m), we recorded the bole char height and the percentage of green, black, and brown foliage.

Following Fernández-García et al. [70], we did not consider CBI attributes related to extended fire severity assessments (e.g., colonizers or the change in species relative abundance) or those that are not representative of Mediterranean ecosystems (e.g., substrate heavy fuel consumption). The attributes were rated in a semiquantitative scale from 0 (no alteration) to 3 (totally altered) from the consensus of at least two observers. The attributes were finally averaged into an integrative CBI value for each plot.

Approximately one year after the fire (June–July 2018), VSC was evaluated in the field using 75 plots of 20 m × 20 m randomly established in relatively homogeneous areas

regarding fire legacies within the wildfire scar (Figure 1) to calibrate and validate VSC retrievals through Sentinel-1 backscatter data. The size of the VSC plots is coincident with the nominal Sentinel-1 resolution. The plots were separated by at least 200 m apart and equally stratified according to the five dominant plant communities of the study site (15 plots per community) by using the classified map. We geolocated the plots in the field through a high-accuracy GPS receiver (RMSEX,Y < 1 m). Four subplots of 2 m × 2 m (azimuths of 45°, 135°, 225°, and 315°, located 6.5 m away from the plot center) were established within each 20 m × 20 m plot to facilitate the vegetation cover estimation as the vertical projected area occupied by vegetation in several strata using a visual estimation method in steps of 5%, following the protocol of Fernández-Guisuraga et al. [36]. We considered the following height strata: (i) herbaceous vegetation (0–0.5 m), low shrubs (0.5–1 m) and tall shrubs (1–4 m) in the understory layer, and intermediate and large trees (>4 m) in the overstory layer [71]. Following Fernández-Guisuraga et al. [36,72], a top-down or a bottom-up procedure was used to estimate vegetation cover depending on the height stratum. The vegetation cover estimates per stratum in the subplots of 2 m × 2 m were averaged to obtain a representative vegetation cover estimate for each plot of 20 m × 20 m. VSC at the plot level was calculated using Shannon's index with appropriate notation [73] (Equation (1)).

$$VSC = -\sum_{i=1}^{S} p_i \ln p_i \quad (1)$$

where p_i is the proportion of vegetation cover corresponding to the ith height stratum and S is the total number of strata in the plot.

2.3. Copernicus Program

The Sentinel-1 (C-band SAR satellite) and Sentinel-2 (multispectral satellite) missions of Copernicus, the joint European Space Agency (ESA)/European Commission Earth observation program previously known as Global Monitoring for Environment and Security (GMES), were used to retrieve wall-to-wall VSC and initial fire severity estimates for the study site, respectively.

2.3.1. Sentinel-1

The Sentinel-1 mission of the Copernicus program comprises a constellation of two polar-orbiting C-band SAR satellites, operating at a wavelength of 5.6 cm (wavelength range of 3.75–7.5 cm) and launched in April 2014 (Sentinel-1A) and April 2016 (Sentinel-1B) for different terrestrial, oceanic, and emergency management applications. The Sentinel-1 twin constellation provides dual polarization capability, a 6-day revisit time at the equator, and is capable of acquiring images in four acquisition modes with different coverages and spatial resolutions, down to 5 m [74]. The Sentinel-1 SAR scene for the study site was acquired from the Copernicus Open Access Hub (https://scihub.copernicus.eu/ accessed on 14 October 2023) on 21st July 2018 at 18:19:41 UTC. The acquisition date was selected on the basis of (i) the peak biomass in the Mediterranean plant communities of the study site, (ii) the closest possible proximity to the end date of the field sampling campaign, and (iii) the absence of precipitation in the 7 days prior to the SAR image acquisition to minimize the distorting effect of vegetation moisture and maximize the effect of vegetation scattering elements on the SAR backscatter [75]. We acquired a SAR Level-1 Ground Range Detected (GRD) product in interferometric wide swath mode at dual polarization (VV vertical-vertical + VH vertical-horizontal) [74]. The Sentinel-1 Toolbox (S1TBX) [76] was used to process the GRD product, including (i) radiometric calibration of VV and VH digital number values to radar brightness (beta nought; β^0), (ii) multi-looking of β^0 VV and VH bands to 20 m, i.e., the nominal Sentinel-1 resolution, (iii) terrain-flattening correction using the algorithm proposed by Small [77] to remove topographic effects and obtain gamma nought (γ^0) backscatter values for VV and VH bands, and (iv) orthorectification of γ^0 VV and VH bands using the range Doppler method [78]. Finally, γ^0 backscatter of VV and VH bands was log-transformed to dB.

2.3.2. Sentinel-2

The Sentinel-2 mission for land monitoring and emergency management comprises a constellation of two polar-orbiting satellites launched in June 2015 (Sentinel-2A) and March 2017 (Sentinel-2B), which feature a 5-day repeat-cycle at the equator. Sentinel-2 MSI is a push-broom sensor that acquires optical spectral data over 13 bands spanning the visible (VIS), near-infrared (NIR), and shortwave infrared (SWIR) regions of the spectrum at different spatial resolutions (four bands at 10 m, six bands at 20 m, and three bands at 60 m) [79]. The Sentinel-2 MSI pre- and post-fire scenes for the study site were also acquired from the Copernicus Open Access Hub (https://scihub.copernicus.eu/ accessed on 14 October 2023) on 13th August 2017 at 11:21:21 UTC (pre-fire) and 2nd September 2017 at 11:21:11 UTC (post-fire). The specific acquisition dates were selected on the basis of the availability of cloud-free scenes closest to start and end dates of the wildfire, meeting the requirements of an initial fire severity assessment. The scenes corresponded to a Level-1C product (top-of-atmosphere reflectance) [79] instead of a Level-2A product already atmospherically corrected for surface reflectance, since Level-2A products have not been systematically distributed by ESA until March 2018. Accordingly, the topographic and atmospheric correction, to obtain a Level-2A product, was implemented through the ATCOR algorithm [80].

Fire severity estimation, as a proxy for the total amount of aboveground biomass consumed [29,81], was conducted using the differenced Normalized Burn Ratio index (dNBR) [82] using band 8A (NIR) and band 12 (SWIR) from the pre and post-fire Sentinel-2 Level-2A scenes (Equations (1) and (3)).

$$NBR = (Band\ 8A - Band\ 12)\ /\ (Band\ 8A + Band\ 12) \quad (2)$$

$$dNBR = 1000\left(NBR_{pre} - NBR_{post}\right) \quad (3)$$

The dNBR was selected in this study because (i) it showed a higher correlation with field-based assessments of fire severity than relativized indices in our study site [83], as determined by internal testing, and (ii) it is the most widely-used approach and a methodological reference in the initial assessments of fire severity [84], including in the Rapid Damage Assessment (RDA) module of the European Forest Fire Information System (EFFIS) (https://effis.jrc.ec.europa.eu/about-effis/ accessed on 22 October 2023).

2.4. Remote Sensing Data Extraction and Analyses

Sentinel-2 dNBR values were extracted for each CBI plot of 20 m × 20 m by averaging the values of a systematically sampled grid of 20 points within each plot (2 m spacing and 2 m apart from the plot edge) in order to account for the mismatch between the Sentinel-2 grid and the plot extent [65,85]. Categorized wall-to-wall fire severity estimates were procured by using the widely-accepted [86–88] CBI thresholds proposed by Miller and Thode [89]: low (CBI < 1.25), moderate (1.25 ≤ CBI ≤ 2.25), and high (CBI > 2.25), which provide comparable fire effects across different Mediterranean plant communities [88]. A linear regression model was used (i) to assess the CBI-dNBR relationship through the coefficient of determination (R^2) and (ii) to categorize wall-to-wall estimates with dNBR fire severity thresholds procured from the model equation. We tested linear and quadratic relationships.

Sentinel-1 γ^0 VV and VH backscatter data were extracted for each VSC field plot of 20 × 20 m following the same approach used for Sentinel-2 dNBR data. Multivariate linear regression was used to model VSC in burned plots (response variable) using, as predictors, Sentinel-1 VV and VH backscatter coefficients. We considered linear and quadratic model terms to account for potential non-linear relationships. Normality and homoscedasticity assumptions of model residuals were evaluated using model diagnostic plots, even though previous studies commonly use a Gaussian distribution to fit vegetation structural diversity models [90]. We assessed the significance of the model from the analysis of variance (ANOVA) output. Model fit was evaluated through the R^2 and the root mean square

error (RMSE). The univariate relationships between VSC and Sentinel-1 backscatter across individual VV and VH polarizations were visualized through scatterplots. The fitted linear model was used to generate wall-to-wall VSC estimates across the study site.

We performed a random stratified sampling of 10,000 points, located at a minimum distance of 100 m, to avoid duplicate points per Sentinel-2 pixel and spatial autocorrelation in the study site [36,47]. The plant community type was used as the strata. For each point, we extracted VSC, categorized fire severity data and the plant community type. A univariate linear mixed model (LMM) and subsequent Tukey's HSD test were fitted to assess whether VSC differs significantly between fire severity scenarios, regardless of the plant community type. Therefore, the response variable was the VSC, and categorized fire severity data was the fixed factor. The community type was included in the LMM as a random factor. Statistical significance was considered at the 0.05 level. Finally, we tested whether the effect of fire severity on VSC was modulated by the plant community type by fitting a multivariate regression model, including the interaction term between fire severity and the plant community type. Tukey' HSD test was used to assess statistical differences between each fire severity category. Statistical significance was considered at the 0.05 level.

All statistical analyses were implemented in R [91].

3. Results

The CBI-dNBR linear regression model showed a high overall fit in the study site (R^2 = 0.841). The relationship was strongly linear (Figure 2), and thus, we did not find a significant improvement in the dNBR fit using a quadratic term (F = 0.256; *p*-value = 0.614). The equation of the linear model and CBI thresholds proposed in the literature were used to establish two dNBR-based fire severity thresholds: low-moderate (dNBR = 384) and moderate-high (dNBR = 659). Most of the wildfire scar was burned at moderate (38.17% of the area) and high (34.35% of the area) fire severity (Figure 1). Using the spatially explicit map of the dominant plant communities in the study site, we determined that *Erica australis*-dominated heathlands and Scots pine forests were the most affected plant communities on the wildfire scale (81% and 80% of their surface area burned at high-severity, respectively). The rest of the plant communities were remarkably less affected, with less than 53% of the area affected by high fire severity.

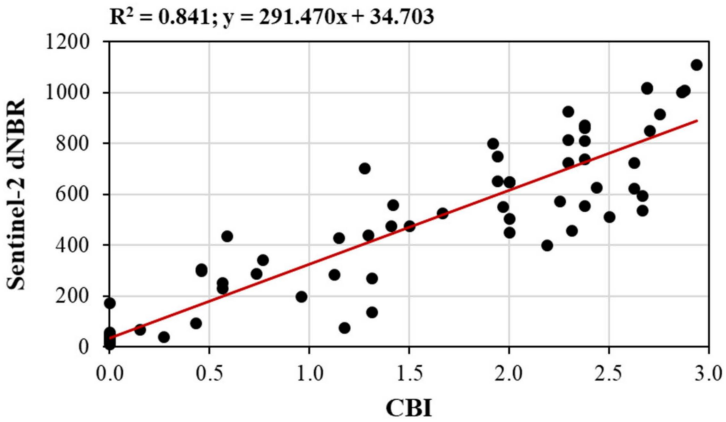

Figure 2. Linear relationship between the difference of the Normalized Burn Ratio index (dNBR) computed from Sentinel-2 MSI pre- and post-fire imagery and the Composite Burn Index (CBI) measured in the field.

The relationships between Sentinel-1 γ^0 VV and VH backscatter data and the field-measured VSC were direct and strongly non-linear (Figure 3). Sentinel-1 γ^0 VH backscatter coefficients showed a stronger correlation with VSC (R^2 = 0.813) than Sentinel-1 γ^0 VV (R^2 = 0.637). Accordingly, Sentinel-1 γ^0 VH backscatter exhibited higher significance in the multivariate linear regression model than VH backscatter (Table 1). Post-fire VSC retrieved from Sentinel-1 backscatter data 1 year after the wildfire featured high fit (R^2 = 0.878) and

low predictive error (RMSE = 0.112) based on the validation with VSC field data. The VSC retrieval was closely adjusted to the 1:1 line without exhibiting significant under- or over-estimation effects throughout the entire field-measured VSC range (Figure 3). Therefore, it can be assumed that the VSC wall-to-wall estimates at the wildfire scale would be reliable.

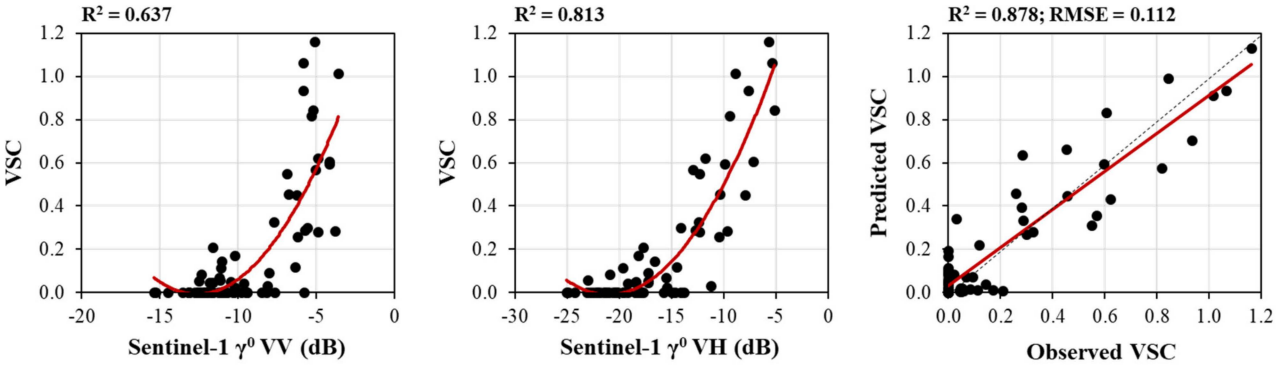

Figure 3. Relationships between Sentinel-1 γ^0 VV and VH backscatter data and field-measured vertical structural complexity (VSC), as well as between the observed and predicted VSC. The dotted black line represents the 1:1 line.

Table 1. Results of the multivariate linear regression model fitted to predict field-measured vertical structural complexity (VSC) from Sentinel-1 γ^0 VV and VH backscatter data. Significant *p*-values are in marked in bold.

Parameter	Estimate	Standard Error	*t*-Value	*p*-Value
Intercept	1.991	0.147	13.542	**<0.001**
VV	0.082	0.020	7.576	**<0.001**
VV²	0.003	0.001	6.092	**<0.001**
VH	0.148	0.036	2.287	**0.025**
VH²	0.004	0.002	1.852	0.068

F = 86.18; *p*-value < 0.001.

Wall-to-wall VSC estimates 1 year after the fire (Figure 4) only partially matched the fire severity spatial variability patterns within the wildfire scar (Figure 1), suggesting a potential modulating effect of the plant community type. The highest VSC estimates were found in valley bottoms, particularly in the western section of the wildfire. The mean VSC value at the study site was 0.298.

Fire severity had a significant effect (F = 228.79; *p*-value < 0.001) on the spatial variability patterns of VSC without considering the influence of plant community types (random factor—in the LMM) (Figure 5). VSC values were significantly higher in low-fire-severity scenarios, while there were no significant differences in the VSC between areas burned at moderate-to-high fire severity (Figure 5).

The effect of fire severity on the VSC showed a different behavior depending on the plant community type (Figure 6), as shown by the significant interaction between both predictors in the linear model (Table 2). The strongest effect was mediated by the plant community type, followed by fire severity and their interaction. Gorse shrublands, dominated by facultative seeders, did not show significant differences in the VSC between fire severity scenarios (Figure 6). The VSC in broom shrublands and Scots pine forests, also dominated by seeder species—obligatory in the case of Scots pine—was significantly higher in areas burned at low fire severity than in areas burned at moderate-to-low severities, where no differences were found between both scenarios (Figure 6). In contrast, communities dominated by resprouter species, i.e., heathlands and Pyrenean oak forests, low and moderate fire severity scenarios showed the highest VSC values with respect to areas burned at high fire severity (Figure 6).

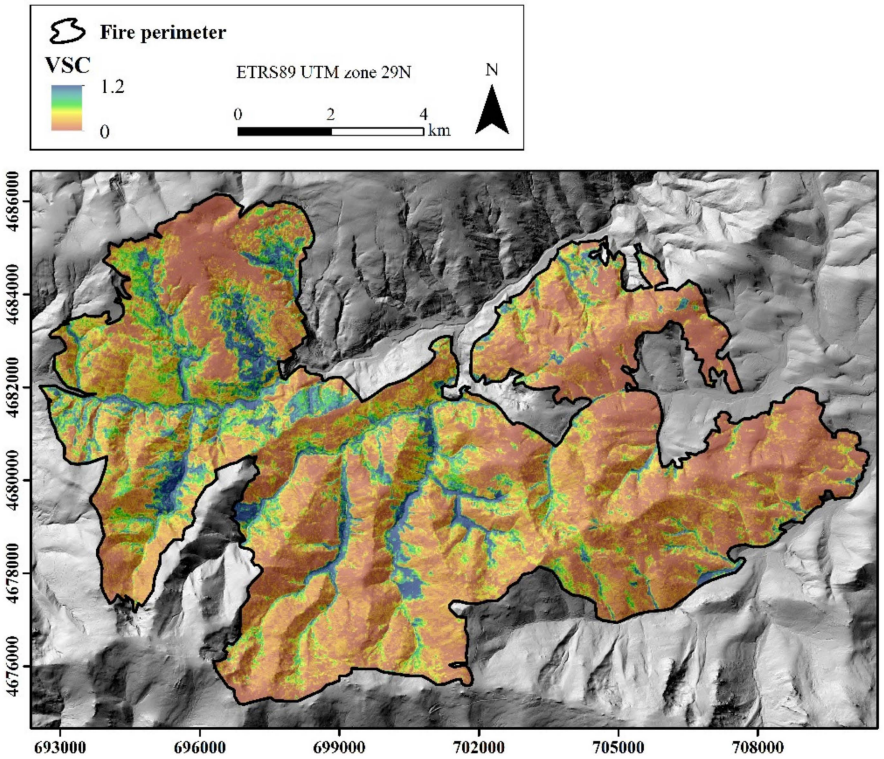

Figure 4. Wall-to-wall estimates of vertical structural complexity (VSC) within the study site computed from Sentinel-1 γ^0 VV and VH backscatter data.

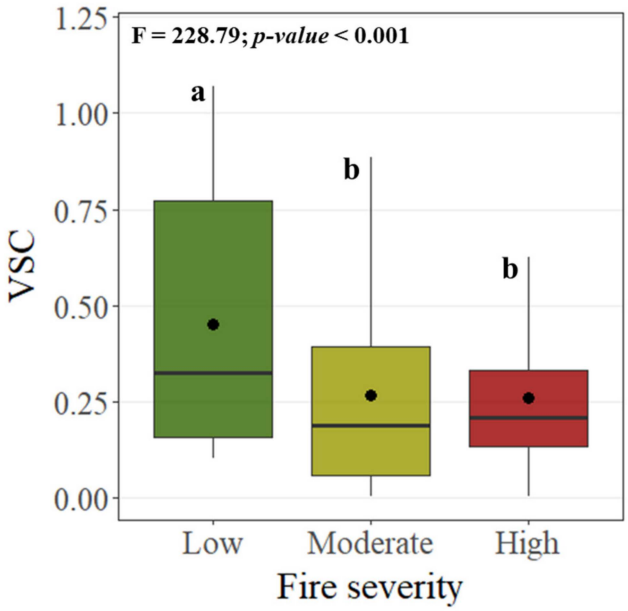

Figure 5. Boxplot depicting the relationship between fire severity and vertical structural complexity (VSC) within the study site. We also show linear mixed model (LMM) results. Lowercase letters in the boxplot denote significant differences at the 0.05 level between fire severity scenarios in Tukey's HSD test.

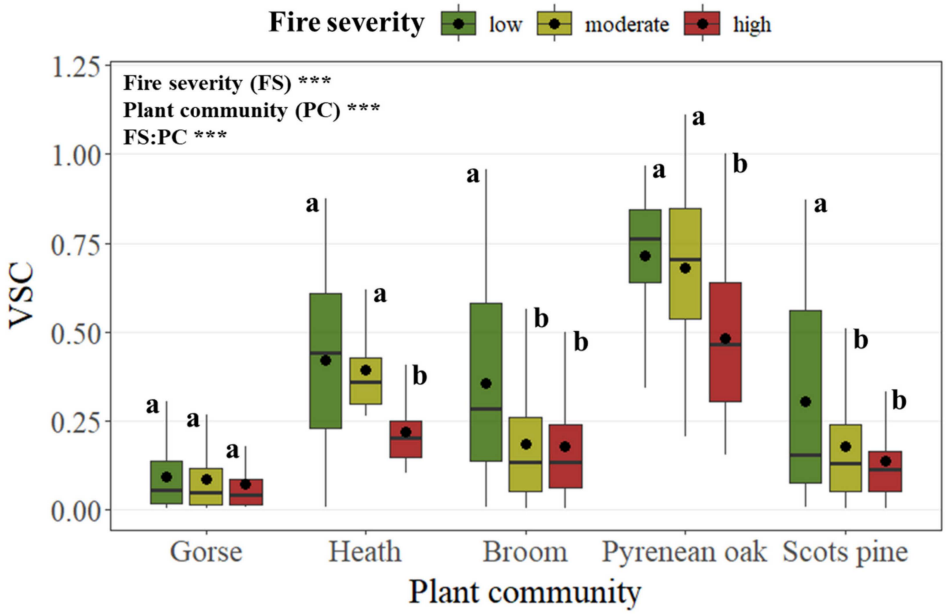

Figure 6. Boxplot depicting the relationship among fire severity, plant community, and vertical structural complexity (VSC) within the study site. We also show linear model results corresponding to those shown in Table 2. Lowercase letters in the boxplot denote significant differences at the 0.05 level between fire severity scenarios in the Tukey's HSD test within each plant community. Significance levels are represented by *** (p-value < 0.001), ** (p-value < 0.01), * (p-value < 0.05), and "none" (p-value > 0.05).

Table 2. Linear regression model results for the effect of fire severity and the plant community type on the vertical structural complexity (VSC). Significant p-values are marked in bold.

Predictor	Df	F	p-Value (>F)
Fire severity	2	345.409	**<0.001**
Plant community	4	4176.961	**<0.001**
Fire severity: Plant community	8	95.752	**<0.001**

4. Discussion

The obtention of wall-to-wall fire severity assessments in fire-prone ecosystems of the western Mediterranean Basin through remote sensing data and techniques that meet management needs in terms of accuracy is of utmost importance (i) to develop reliable post-fire management plans and strategies [29,81,92] and (ii) to improve the understanding about the ecological implications of fire regime shifts on post-fire succession pathways and ecosystem functions in the context of global change [36,93]. Previous research reported that VSC monitoring is also essential for this purpose in fire-prone burned landscapes [4,39,47]. The results of the present study have contributed, for the first time, to shed light into the relationship between fire severity and the VSC spatial variability. Remarkably, the sound ecological relationships found between both factors for each plant community would allow forest managers to implement management interventions targeted at recovering VSC in fire-prone ecosystems by considering only wall-to-wall fire severity estimates using passive optical sensors, which are simpler to produce than vegetation structural estimates from SAR data.

Sentinel-1 SAR backscatter data successfully captured three-dimensional vegetation structural characteristics in this study and thus the VSC spatial variability in the short-term after fire. This can be attributed to the high sensitivity of SAR data to the density and size of stems, branches, and foliage in the canopy [52], as compared to passive optical data [63]. In contrast, field-measured biomass consumption through the CBI could be accurately

modeled using the dNBR index calculated from Sentinel-2 passive optical data because of the NIR and SWIR sensitivity of broadband spectral indices to top-of-canopy char and vegetation consumption in post-fire environments [94], as previously reported in many studies worldwide [70,84,92,95]. This is particularly evident if the fire effects are correlated among vegetation strata [96], as in our study site.

Remarkably, the dNBR threshold for moderate–high severity, with particular relevance in post-fire management, was comparable to those reported in other Mediterranean sites [89,97,98]. Previous research also evidenced that reduced canopy closure due to foliage consumption in several Mediterranean forest and shrub plant communities across the Iberian Peninsula enabled the penetration and interaction of short-wavelength SAR signal with the lower vegetation strata [75,99]. In areas burned at low fire severity, and thus with a higher density of unconsumed foliage, the SAR signal may be related to fire-induced changes in the canopy architecture [100], which may also act as a proxy for structural density in subcanopy strata [101].

The direct relationship between VSC and Sentinel-1 C-band SAR backscatter data, evidenced in this study, is consistent with the reduction in the γ^0 VV and VH backscatter intensity as the number of scattering elements in the canopy decreases [63,99]. Fernández-Guisuraga et al. [47] also evidenced a similar relationship in the study site, but the authors estimated VSC from the data fusion of Sentinel-1 C-band SAR backscatter and Sentinel-2 reflectance, which may hinder model transferability because of the plant-community-dependent behavior of passive optical data as a proxy for canopy traits [98]. Indeed, the overall accuracy of the VSC estimates was considerably higher in the present study (R^2 = 0.878 vs. R^2 = 0.810). The high overall fit, and thus generalization ability of SAR-based VSC estimates considering the different plant communities in the study site, could be explained by the physical basis of SAR data to characterize the variability in the volumetric, crown, and dihedral scattering in burned areas [64]. In this context, cross-polarized C-band data (VH polarization) featured the strongest correlation with VSC in this study, which may be associated with the domination of cross-polarized waves by volumetric scattering from the canopy branches, tree density, and tree height [63,102] and thus may be more responsive to VSC variability. Altogether, our results suggest that this approach could be leveraged in other Mediterranean plant communities and those of other biomes exhibiting low-to-moderate canopy closure that allows for the penetration of short-wavelength SAR signal [75,103], without undergoing limitations exerted by airborne LiDAR data availability. Also, the link evidenced here between the VSC response, as modulated by fire severity and the plant community type, could be extrapolated to a wide variety of Mediterranean plant communities. Future studies could also leverage the potential of GEDI and ICESat-2 laser altimeters, where available, to supplement SAR data based on the calculation of height-distribution metrics within the plant communities [104].

The large extensions of Scots pine forests and heathlands burned at high fire severity is consistent with previous research. Unmanaged Scots pine forests are highly prone to extreme fire behavior because of ladder fuels with high crowning potential [105]. Indeed, *Pinus sylvestris* is moderately fire resistant [32] and one of the most susceptible European pine species to crown fires [106]. The large amount of live and dead fuel, particularly close to the ground, and the homogeneous horizontal structure and even-aged stand characteristics related to the vertical structure make heathlands dominated by Erica australis prone to extreme fire behavior [107–109].

Our study provides clear evidence that fire severity, regardless of the plant community type, may lead to significant changes in the physical arrangement of the vegetation in the vertical canopy profile. The simplification in structural diversity at the plant community level has been previously reported in the mesic and dry sclerophyll forests of southeastern Australia that burned at high fire severity [110,111], being attributed to long-lasting impacts of elevated vegetation mortality under Mediterranean climate conditions [112]. The same behavior was evidenced by Kane et al. [57] in several forest types and woodlands within the Yosemite National Park, where high-severity patches featured the least structural

heterogeneity because open spatial structures clearly dominated. Conversely, previous research also reported the dominance of more structurally diverse and fragmented canopies following high-intensity crown fires in the short-term after fire in Mediterranean maritime pine (*Pinus pinaster* Ait.) stands and mixed-forests [56]. The authors reported that severe wildfires enhanced the vegetation cover evenness by height strata over the early post-fire period, but the effect diminished in the medium-term because of the increasing dominance of recovering resprouter species. The large variability in the effects of fire severity on vegetation structural characteristics is consistent with our results showing that plant community types strongly modulated the VSC response to increasing fire severity even within the same wildfire. Also, this response was strongly linked to the regenerative strategies of the dominant species in the community (i.e., seedling recruitment and resprouting response).

The aerial and soil seed banks of the most susceptible seeder species to crown damage, such as dense broom stands and Scots pine forests [68], can be seriously hindered by moderate-to-severe wildfires [113], triggering the seed bank depletion and precluding seedling recruitment [114–116]. In this context, the shrub aerial parts are particularly vulnerable to fire because of their growth-form close to the soil and the associated heat-induced impacts on cambial tissues and roots [117–119], even at moderate severities [36]. For its part, the smaller individuals in moderately fire-resistant Scots pine forests are only capable of surviving low-intensity wildfires [32]. The recovery trajectories in Scots pine forests after a high-intensity wildfire rely on seed dispersal from unburned islands [120], with a limited seeding and resprouting response of the accompanying understory species under this scenario [121]. These limited post-fire recovery responses, together with high biomass consumption, could explain the strong impact of moderate-to-high fire severity on the VSC of broom shrublands and Scots pine forests, dominated by facultative and obligate seeder species, respectively. This behavior was amplified in gorse shrublands, dominated also by facultative seeders, which exhibited a small VSC that did not differ between fire severity scenarios. This can be probably associated with the poor environmental conditions of the sites where gorse communities are established, such as degraded soils with low soil organic carbon and available nutrient contents after the wildfire [122], hindering vegetation recovery responses in the short-term after the fire at the study site [8].

In contrast, moderate fire severity did not have a stronger impact on VSC than low severity in communities dominated by resprouter species, i.e., heathlands and Pyrenean oak forests, which are precisely those exhibiting the highest VSC under all fire severity scenarios. The strong resprouting response of the dominant species of both plant communities [47,123] allows for the rapid recovery of below- and above-ground plant biomass [124]. In addition, only the fire impact on bud-forming tissues of resprouter species is expected to hinder resprouting vigor and delay the resprouting response at high fire severity [125–127]. In the specific case of Pyrenean oak forests, typically located in moister microclimates [128], canopy re-establishment may be enhanced under lower environmental stress conditions in the short-term after the fire.

Future research should confirm the plant community-dependent VSC trends evidenced here by using a long-term monitoring approach to account for delayed post-fire mortality effects and potential changes in the species composition [105]. In addition, the potential effect of fire history attributes on VSD recovery trajectories [25,53,54], including the fire frequency and time since the last fire, should be evaluated on large spatial scales in fire-prone ecosystems of the western Mediterranean Basin by leveraging the remote sensing-based approach proposed here.

5. Conclusions

The results of this study shed light, for the first time, into the relationships between fire severity and the VSC spatial variability, as modulated by the plant community type in Mediterranean fire-prone ecosystems. The physical sense and sensitivity of C-band SAR backscatter data to the variability of the density and distribution of scattering elements in burned vegetation canopies, including stems, branches, and foliage, allowed for accurate

VSC predictions considering the high variability in the three-dimensional structure of the studied plant communities. Our results suggest that the effects of fire severity on vegetation structural characteristics were strongly modulated by the plant community type in the short-term after fire. The VSC response was strongly linked to the regenerative strategies of the dominant species in the community. In this context, the impact of fire severity on VSC was stronger in communities dominated by seeder species than in those dominated by resprouting species with strong recovery responses, even just one year after the fire. Future research should confirm, in the long term, the trends observed here, as well as the transferability of our approach to other types of Mediterranean plant communities and in other biomes.

Author Contributions: Conceptualization, J.M.F.-G.; Methodology, L.J.-L., E.M. and J.M.F.-G.; Software, J.M.F.-G.; Formal Analysis, L.J.-L.; Investigation, L.J.-L., E.M. and J.M.F.-G.; Resources, E.M.; Data Curation, L.J.-L. and J.M.F.-G.; Writing—Original Draft Preparation, L.J.-L.; Writing—Review & Editing, E.M. and J.M.F.-G.; Supervision, J.M.F.-G.; Project Administration, E.M. and J.M.F.-G.; Funding Acquisition, E.M. and J.M.F.-G. All authors have read and agreed to the published version of the manuscript.

Funding: This study was financially supported by the Spanish Ministry of Science and Innovation in the framework of the LANDSUSFIRE project (PID2022-139156OB-C21) within the National Program for the Promotion of Scientific-Technical Research (2021–2023), and with Next-Generation Funds of the European Union (EU) in the framework of the FIREMAP project (TED2021-130925B-I00); by the Regional Government of Castile and León in the framework of the IA-FIREXTCyL project (LE081P23); and by National Funds from FCT—Portuguese Foundation for Science and Technology, under the project UIDB/04033/2020. José Manuel Fernández-Guisuraga was supported by a Ramón Areces Foundation postdoctoral fellowship.

Institutional Review Board Statement: Not applicable.

Informed Consent Statement: Not applicable.

Data Availability Statement: The data presented in this study are available on request from the corresponding author.

Conflicts of Interest: The authors declare no conflict of interest.

References

1. Fernández-García, V.; Beltrán-Marcos, D.; Fernández-Guisuraga, J.M.; Marcos, E.; Calvo, L. Predicting potential wildfire severity across Southern Europe with global data sources. *Sci. Total Environ.* **2022**, *829*, 154729. [CrossRef]
2. Ninyerola, M.; Pons, X.; Roure, J.M. *Atlas Climático Digital de la Península Ibérica. Methodology and Applications in Bioclimatology and Geobotany*; Autonomous University of Barcelona: Barcelona, Spain, 2005.
3. Pausas, J.G.; Llovet, J.; Rodrigo, A.; Vallejo, R. Are wildfires a disaster in the Mediterranean basin? A review. *Int. J. Wildland Fire* **2008**, *17*, 713–723. [CrossRef]
4. González-De Vega, S.; De las Heras, J.; Moya, D. Resilience of Mediterranean terrestrial ecosystems and fire severity in semiarid areas: Responses of Aleppo pine forests in the short, mid and long term. *Sci. Total Environ.* **2016**, *573*, 1171–1177. [CrossRef]
5. Ribeiro, L.M.; Viegas, D.X.; Almeida, M.; McGee, T.K.; Pereira, M.G.; Parente, J.; Xanthopoulos, G.; Leone, V.; Mariano, G.; Hardin, H. 2—Extreme wildfires and disasters around the world: Lessons to be learned. In *Extreme Wildfire Events and Disasters*; Tedim, F., Leone, V., McGee, T.K., Eds.; Elsevier: Amsterdam, The Netherlands, 2020; pp. 31–51.
6. Fernández-Guisuraga, J.M.; Suárez-Seoane, S.; Calvo, L. Modeling Pinus pinaster forest structure after a large wildfire using remote sensing data at high spatial resolution. *For. Ecol. Manag.* **2019**, *446*, 257–271. [CrossRef]
7. Grau-Andrés, R.; Davies, G.M.; Waldron, S.; Scott, E.M.; Gray, A. Increased fire severity alters initial vegetation regeneration across Calluna-dominated ecosystems. *J. Environ. Manag.* **2019**, *231*, 1004–1011. [CrossRef]
8. Huerta, S.; Marcos, E.; Fernández-García, V.; Calvo, L. Resilience of Mediterranean communities to fire depends on burn severity and type of ecosystem. *Fire Ecol.* **2022**, *18*, 28. [CrossRef]
9. Certini, G. Effects of fire on properties of forest soils: A review. *Oecologia* **2005**, *143*, 1–10. [CrossRef]
10. Mataix-Solera, J.; Cerdà, A.; Arcenegui, V.; Jordán, A.; Zavala, L.M. Fire effects on soil aggregation: A review. *Earth Sci. Rev.* **2011**, *109*, 44–60. [CrossRef]
11. Costa, P.; Castellnou, M.; Larrañaga, A.; Miralles, M.; Kraus, P.D. *Prevention of Large Wildfires Using the Fire Types Concept*; Unitat Tècnica del GRAF: Barcelona, Spain, 2011.

12. Fernández-García, V.; Marcos, E.; Fernández-Guisuraga, J.M.; Taboada, S.; Suárez-Seoane, S.; Calvo, L. Impact of burn severity on soil properties in a Pinus pinaster ecosystem immediately after fire. *Int. J. Wildland Fire* **2019**, *28*, 354–364. [CrossRef]
13. Inbar, A.; Lado, M.; Sternberg, M.; Tenau, H.; Ben-Hur, M. Forest fire effects on soil chemical and physicochemical properties, infiltration, runoff, and erosion in a semiarid Mediterranean region. *Geoderma* **2014**, *221*, 131–138. [CrossRef]
14. Lucas-Borja, M.E.; Plaza-Álvarez, P.A.; Gonzalez-Romero, J.; Sagra, J.; Alfaro-Sánchez, R.; Zema, D.A.; Moya, D.; de las Heras, J.; 2019. Short-term effects of prescribed burning in Mediterranean pine plantations on surface runoff, soil erosion and water quality of runoff. *Sci. Total Environ.* **2019**, *674*, 615–622. [CrossRef]
15. Rutigliano, F.A.; Migliorini, M.; Maggi, O.; D'Ascoli, R.; Fanciulli, P.P.; Persiani, A.M. Dynamics of fungi and fungivorous microarthropods in a Mediterranean maquis soil affected by experimental fire. *Eur. J. Soil Biol.* **2013**, *56*, 33–43. [CrossRef]
16. Cunillera-Montcusí, D.; Gascón, S.; Tornero, I.; Sala, J.; Àvila, N.; Quintana, X.D.; Boix, D. Direct and indirect impacts of wildfire on faunal communities of Mediterranean temporary ponds. *Freshw. Biol.* **2019**, *64*, 323–334. [CrossRef]
17. Peñuelas, J.; Lloret, F.; Montoya, R. Severe drought effects on Mediterranean woody flora in Spain. *For. Sci.* **2001**, *47*, 214–218.
18. Myers, N.; Mittermeier, R.; Mittermeier, C.; Fonseca, G.A.B.; Kent, J. Biodiversity hotspots for conservation priorities. *Nature* **2000**, *403*, 853–858. [CrossRef]
19. Rodrigues, M.; Camprubí, A.C.; Balaguer-Romano, R.; Ruffault, J.; Fernandes, P.M.; Resco de Rios, V. Drivers and implications of the extreme 2022 wildfire season in Southwest Europe. *Sci. Total Environ.* **2023**, *859*, 160320. [CrossRef]
20. Turner, M.G. Disturbance and landscape dynamics in a changing world. *Ecology* **2010**, *91*, 2833–2849. [CrossRef]
21. Moreira, F.; Viedma, O.; Arianoutsou, M.; Curt, T.; Koutsias, N.; Rigolot, E.; Barbati, A.; Corona, P.; Vaz, P.; Xanthopoulos, G.; et al. Landscape—Wildfire interactions in southern Europe: Implications for landscape management. *J. Environ. Manag.* **2011**, *92*, 2389–2402. [CrossRef]
22. Jones, M.J.; Abatzoglou, J.T.; Veraverbeke, S.; Andela, N.; Lasslop, G.; Forkel, M.; Smith, J.P.A.; Burton, C.; Betts, A.B.; van der Werf, R.G.; et al. Global and Regional Trends ans Drivers of Fire Under Climate Change. *Rev. Geophys.* **2022**, *60*, e2020RG000726. [CrossRef]
23. Mataix-Solera, J.; Cerdà, A. Incendios forestales en España. Ecosistemas terrestres y suelos. In *Efectos de Los Incendios Forestales Sobre los Suelos en España*; Cerdà, A., Mataix-Solera, J., Eds.; Cátedra Divulgación de la Ciencia, Universitat de València: Valencia, Spain, 2009; pp. 13–53.
24. Seidl, R.; Rammer, W.; Spies, T.A. Disturbance legacies increase the resilience of forest ecosystem structure, composition, and functioning. *Ecol. Appl.* **2014**, *24*, 2063–2077. [CrossRef]
25. Johnstone, J.F.; Allen, C.D.; Franklin, J.F.; Frelich, L.E.; Harvey, B.J.; Higuera, P.E.; Mack, M.C.; Meentemeyer, R.K.; Metz, M.R.; Perry, G.L.W.; et al. Changing disturbance regimes, ecological memory, and forest resilience. *Front. Ecol. Environ.* **2016**, *14*, 369–378. [CrossRef]
26. Doblas-Miranda, E.; Alonso, R.; Arnan, X.; Bermejo, V.; Brotons, L.; Heras, J.d.L.; Estiarte, M.; Hódar, J.; Llorens, P.; Lloret, F.; et al. A review of the combination among global change factors in forests, shrublands and pastures of the Mediterranean Region: Beyond drought effects. *Glob. Planet. Change* **2017**, *148*, 42–54. [CrossRef]
27. Turetsky, M.R.; Baltzer, J.L.; Johnstone, J.F.; Mack, M.C.; McCann, K.; Schuur, E.A.G. Losing legacies, ecological release, and transient responses: Key challenges for the future of northern ecosystem science. *Ecosystems* **2017**, *20*, 23–30. [CrossRef]
28. Lentile, L.B.; Holden, Z.A.; Smith, A.M.S.; Falkowski, M.J.; Hudak, A.T.; Morgan, P.; Lewis, S.A.; Gessler, P.E.; Benson, N.C. Remote sensing techniques to assess active fire characteristics and post-fire effects. *Int. J. Wildland Fire* **2006**, *15*, 319–345. [CrossRef]
29. Keeley, J.E. Fire intensity, fire severity and burn severity: A brief review and suggested usage. *Int. J. Wildland Fire* **2009**, *18*, 116–126. [CrossRef]
30. Archibald, S.; Lehmann, C.E.R.; Belcher, C.M.; Bond, W.J.; Bradstock, R.A.; Daniau, A.L.; Dexter, K.G.; Forrestel, E.J.; Greve, M.; He, T. Biological and geophysical feedbacks with fire in the Earth system. *Environ. Res. Lett.* **2018**, *13*, 033003. [CrossRef]
31. Calvo, L.; Santalla, S.; Valbuena, L.; Marcos, E.; Tárrega, R.; Luis-Calabuig, E. Post-fire natural regeneration of a *Pinus pinaster* forest in NW Spain. *Plant Ecol.* **2008**, *197*, 81–90. [CrossRef]
32. Fernandes, P.M.; Vega, J.A.; Jimenez, E.; Rigolot, E. Fire resistance of European pines. *For. Ecol. Manag.* **2008**, *256*, 246–255. [CrossRef]
33. Fernández-Guisuraga, J.M.; Calvo, L.; Suárez-Seoane, S. Monitoring post-fire neighborhood competition effects on pine saplings under different environmental conditions by means of UAV multispectral data and structure-from-motion photogrammetry. *J. Environ. Manag.* **2022**, *305*, 114373. [CrossRef]
34. López-Poma, R.; Bautista, S. Plant regeneration functional groups modulate the response to fire of soil enzyme activities in a Mediterranean shrubland. *Soil Biol. Biochem.* **2014**, *79*, 5–13. [CrossRef]
35. Santín, C.; Doerr, S.H. Fire effects on soils: The human dimension. *Philos. Trans. R. Soc. B* **2016**, *371*, 20150171. [CrossRef]
36. Fernández-Guisuraga, J.M.; Suárez-Seoane, S.; Calvo, L. Radiative transfer modeling to measure fire impact and forest engineering resilience at short-term. *ISPRS J. Photogramm. Remote Sens.* **2021**, *176*, 30–41. [CrossRef]
37. Gunderson, L.H.; Holling, C.S. *Panarchy: Understanding Transformations in Human and Natural Systems*; Island Press: Washington, DC, USA, 2002.
38. Newton, A.C.; Cantarello, E. Restoration of forest resilience: An achievable goal? *New For.* **2015**, *46*, 645–668. [CrossRef]

39. Chergui, B.; Fahd, S.; Santos, X.; Pausas, J.G. Socioeconomic factors drive fire-regime variability in the Mediterranean Basin. *Ecosystems* **2018**, *21*, 619–628. [CrossRef]
40. Drever, C.R.; Peterson, G.; Messier, C.; Bergeron, Y.; Flannigan, M. Can forest management based on natural disturbances maintain ecological resilience? *Can. J. For. Res.* **2006**, *36*, 2285–2299. [CrossRef]
41. Gara, T.W.; Darvishzadeh, R.; Skidmore, A.K.; Wang, T. Impact of vertical canopy position on leaf spectral properties and traits across multiple species. *Remote Sens.* **2018**, *10*, 346. [CrossRef]
42. LaRue, E.A.; Hardiman, B.S.; Elliott, J.M.; Fei, S. Structural diversity as a predictor of ecosystem function. *Environ. Res. Lett.* **2019**, *14*, 114011. [CrossRef]
43. Gough, C.M.; Atkins, J.W.; Fahey, R.T.; Hardiman, B.S. High rates of primary production in structurally complex forests. *Ecology* **2019**, *100*, e02864. [CrossRef]
44. Wood, E.M.; Pidgeon, A.M.; Radeloff, V.C.; Keuler, N.S. Image texture as a measure of vegetation structure using remote sensing. *Remote Sens. Environ.* **2012**, *121*, 516–526. [CrossRef]
45. Southwood, T.R.E.; Brown, V.K.; Reader, P.M. The relationships of plant and insect diversities in succession. *Biol. J. Linn. Soc.* **1979**, *12*, 327–348. [CrossRef]
46. Rotenberry, J.T.; Wiens, J.A. Habitat structure, patchiness, and avian communities in North American steppe vegetation: A multivariate analysis. *Ecology* **1980**, *61*, 1228–1250. [CrossRef]
47. Fernández-Guisuraga, J.M.; Suárez-Seoane, S.; Calvo, L. Radar and multispectral remote sensing data accurately estimate vegetation vertical structure diversity as a fire resilience indicator. *Remote Sens. Ecol. Conserv.* **2023**, *9*, 117–132. [CrossRef]
48. Fernández-Guisuraga, J.M.; Calvo, L.; Suárez-Seoane, S. Comparison of pixel unmixing models in the evaluation of post-fire forest resilience based on temporal series of satellite imagery at moderate and very high spatial resolution. *ISPRS J. Photogramm. Remote Sens.* **2020**, *164*, 217–228. [CrossRef]
49. Suárez-Seoane, S.; Osborne, P.E.; Baudry, J. Responses of birds of different biogeographic origins and habitat requirements to agricultural land abandonment in northern Spain. *Biol. Conserv.* **2002**, *105*, 333–344. [CrossRef]
50. Santana, J.; Porto, M.; Reino, L.; Beja, P. Long-term understory recovery after mechanical fuel reduction in Mediterranean cork oak forests. *For. Ecol. Manag.* **2011**, *261*, 447–459. [CrossRef]
51. Meeussen, C.; Govaert, S.; Vanneste, T.; Calders, K.; Bollmann, K.; Brunet, J.; Cousins, S.A.O.; Diekmann, M.; Graae, B.J.; Hedwall, P.O.; et al. Structural variation of forest edges across Europe. *For. Ecol. Manag.* **2020**, *462*, 117929. [CrossRef]
52. Bergen, K.M.; Goetz, S.J.; Dubayah, R.O.; Henebry, G.M.; Hunsaker, C.T.; Imhoff, M.L.; Nelson, R.F.; Parker, G.G.; Radeloff, V.C. Remote sensing of vegetation 3D structure for biodiversity and habitat: Review and implications for lidar and radar spaceborne missions. *J. Geophys. Res. Biogeosciences* **2009**, *114*, G00E06. [CrossRef]
53. Fontaine, J.B.; Donato, D.C.; Robinson, W.D.; Law, B.E.; Kauffman, J.B. Bird communities following high-severity fire: Response to single and repeat fires in a mixed-evergreen forest, Oregon, USA. *For. Ecol. Manag.* **2009**, *257*, 1496–1504. [CrossRef]
54. Foster, C.N.; Barton, P.S.; Robinson, N.M.; MacGregor, C.I.; Lindenmayer, D.B. Effects of a large wildfire on vegetation structure in a variable fire mosaic. *Ecol. Appl.* **2017**, *27*, 2369–2381.615. [CrossRef]
55. Lydersen, J.M.; Collins, B.M.; Miller, J.D.; Fry, D.L.; Stephens, S.L. Relating Fire-Caused Change in Forest Structure to Remotely Sensed Estimates of Fire Severity. *Fire Ecol.* **2016**, *12*, 99–116. [CrossRef]
56. Marzano, R.; Lingua, E.; Garbarino, M. Post-fire effects and short-term regeneration dynamics following high-severity crown fires in a Mediterranean forest. *iForest* **2012**, *5*, 93–100. [CrossRef]
57. Kane, V.R.; North, M.P.; Lutz, J.A.; Churchill, D.J.; Roberts, S.L.; Smith, D.F.; McGaughey, R.J.; Kane, J.T.; Brooks, M.L. Assessing fire effects on forest spatial structure using a fusion of Landsat and airborne LiDAR data in Yosemite National Park. *Remote Sens. Environ.* **2014**, *151*, 89–101. [CrossRef]
58. Yin, C.; He, B.; Yebra, M.; Quan, X.; Edwards, A.C.; Liu, X.; Liao, Z. Improving burn severity retrieval by integrating tree canopy cover into radiative transfer model simulation. *Remote Sens. Environ.* **2020**, *236*, 111454. [CrossRef]
59. Vila, G.; Barbosa, P. Post-fire vegetation regrowth detection in the Deiva Marina region (Liguria-Italy) using Landsat TM and ETM+ data. *Ecol. Model.* **2010**, *221*, 75–84. [CrossRef]
60. Ireland, G.; Petropoulos, G.P. Exploring the relationships between post-fire vegetation regeneration dynamics, topography and burn severity: A case study from the Montane Cordillera Ecozones of Western Canada. *Appl. Geogr.* **2015**, *56*, 232–248. [CrossRef]
61. Fernandez-Manso, A.; Quintano, C.; Roberts, D.A. Burn severity influence on post-fire vegetation cover resilience from Landsat MESMA fraction images time series in Mediterranean forest ecosystems. *Remote Sens. Environ.* **2016**, *184*, 112–123. [CrossRef]
62. Fernández-Guisuraga, J.M.; Suárez-Seoane, S.; Fernandes, P.M.; Fernández-García, V.; Fernández-Manso, A.; Quintano, C.; Calvo, L. Pre-fire aboveground biomass, estimated from LiDAR, spectral and field inventory data, as a major driver of burn severity in maritime pine (*Pinus pinaster*) ecosystems. *For. Ecosyst.* **2022**, *9*, 100022. [CrossRef]
63. Tanase, M.A.; Kennedy, R.; Aponte, C. Radar Burn Ratio for fire severity estimation at canopy level: An example for temperate forests. *Remote Sens. Environ.* **2015**, *170*, 14–31. [CrossRef]
64. Kalogirou, V.; Ferrazzoli, P.; Vecchia, A.D.; Foumelis, M. On the SAR Backscatter of Burned Forests: A Model-Based Study in C-Band, Over Burned Pine Canopies. *IEEE Trans. Geosci. Remote Sens.* **2014**, *52*, 6205–6215. [CrossRef]
65. Fernández-Guisuraga, J.M.; Marcos, E.; Suárez-Seoane, S.; Calvo, L. ALOS-2 L-band SAR backscatter data improves the estimation and temporal transferability of wildfire effects on soil properties under different post-fire vegetation responses. *Sci. Total Environ.* **2022**, *842*, 156852. [CrossRef]

66. Fernandes, P.M. Fire-smart management of forest landscapes in the Mediterranean basin under global change. *Landsc. Urban Plan.* **2013**, *110*, 175–182. [CrossRef]
67. Strahler, A.H. The use of prior probabilities in maximum likelihood classification of remotely sensed data. *Remote Sens. Environ.* **1980**, *10*, 135–163. [CrossRef]
68. Fernández-Guisuraga, J.M.; Suárez-Seoane, S.; García-Llamas, P.; Calvo, L. Vegetation structure parameters determine high burn severity likelihood in different ecosystem types: A case study in a burned Mediterranean landscape. *J. Environ. Manag.* **2021**, *288*, 112462. [CrossRef]
69. Key, C.H.; Benson, N. Landscape assessment: Ground measure of severity, the Composite Burn Index; and remote sensing of severity, the Normalized Burn Ratio. In *FIREMON: Fire Effects Monitoring and Inventory System*; Lutes, D.C., Keane, R.E., Caratti, J.F., Key, C.H., Benson, N.C., Gangi, L.J., Eds.; General Technical Report RMRS-GTR-164; USDA Forest Service, Rocky Mountain Research Station: Ogden, UT, USA, 2005; pp. CD:LA1–LA51.
70. Fernández-García, V.; Santamarta, M.; Fernández-Manso, A.; Quintano, C.; Marcos, E.; Calvo, L. Burn severity metrics in fire-prone pine ecosystems along a climatic gradient using Landsat imagery. *Remote Sens. Environ.* **2018**, *206*, 205–217. [CrossRef]
71. Casenave, J.L.; Pelotto, J.P.; Protomastro, J. Edge-interior differences in vegetation structure and composition in a Chaco semi-arid forest, Argentina. *For. Ecol. Manag.* **1995**, *72*, 61–69. [CrossRef]
72. Fernández-Guisuraga, J.M.; Verrelst, J.; Calvo, L.; Suárez-Seoane, S. Hybrid inversion of radiative transfer models based on high spatial resolution satellite reflectance data improves fractional vegetation cover retrieval in heterogeneous ecological systems after fire. *Remote Sens. Environ.* **2021**, *255*, 112304. [CrossRef]
73. Angelo, J.J. Characterizing the Vertical Structure and Structural Diversity of Florida Oak Scrub Vegetation Using Discrete-Return LiDAR. Master's Thesis, University of Central Florida, Orlando, FL, USA, 2010.
74. ESA. Sentinel-1 SAR User Guide. 2023. Available online: https://sentinel.esa.int/web/sentinel/user-guides/sentinel-1-sar (accessed on 14 October 2023).
75. Belenguer-Plomer, M.A.; Tanase, M.A.; Fernandez-Carrillo, A.; Chuvieco, E. Burned area detection and mapping using Sentinel-1 backscatter coefficient and thermal anomalies. *Remote Sens. Environ.* **2019**, *233*, 111345. [CrossRef]
76. ESA. The Sentinel-1 Toolbox. 2023. Available online: https://sentinel.esa.int/web/sentinel/toolboxes/sentinel-1 (accessed on 14 October 2023).
77. Small, D. Flattening gamma: Radiometric terrain correction for SAR imagery. *IEEE Trans. Geosci. Remote Sens.* **2011**, *49*, 3081–3093. [CrossRef]
78. Small, D.; Schubert, A. *Guide to ASAR Geocoding, RSL-ASAR-GC-AD, Issue 1.0*; University of Zurich: Zurich, Switzerland, 2008.
79. ESA. Sentinel-2 MSI User Guide. 2023. Available online: https://sentinel.esa.int/web/sentinel/user-guides/sentinel-2-msi (accessed on 14 October 2023).
80. Richter, R.; Schläpfer, D. *Atmospheric/Topographic Correction for Satellite Imagery*; DLR Report DLR-IB 565-01/2018; ReSe Applications Schläpfer: Wil, Switzerland, 2018.
81. Morgan, P.; Keane, R.E.; Dillon, G.K.; Jain, T.B.; Hudak, A.T.; Karau, E.C.; Sikkink, P.G.; Holden, Z.A.; Strand, E.K. Challenges of assessing fire and burn severity using field measures, remote sensing and modelling. *Int. J. Wildland Fire* **2014**, *23*, 1045–1060. [CrossRef]
82. Key, C.H. Ecological and sampling constraints on defining landscape fire severity. *Fire Ecol.* **2006**, *2*, 34–59. [CrossRef]
83. García-Llamas, P.; Suárez-Seoane, S.; Fernández-Manso, A.; Quintano, C.; Calvo, L. Evaluation of fire severity in fire prone-ecosystems of Spain under two different environmental conditions. *J. Environ. Manag.* **2020**, *271*, 110706. [CrossRef]
84. Soverel, N.O.; Perrakis, D.D.B.; Coops, N.C. Estimating burn severity from Landsat dNBR and RdNBR indices across western Canada. *Remote Sens. Environ.* **2010**, *114*, 1896–1909. [CrossRef]
85. Picotte, J.J.; Robertson, K.M. Validation of remote sensing of burn severity in south-eastern US ecosystems. *Int. J. Wildland Fire* **2011**, *20*, 453–464. [CrossRef]
86. Parks, S.A.; Dillon, G.K.; Miller, C. A new metric for quantifying burn severity: The relativized burn ratio. *Remote Sens.* **2014**, *6*, 1827–1844. [CrossRef]
87. Stambaugh, M.C.; Hammer, L.D.; Godfrey, R. Performance of burn-severity metrics and classification in oak woodlands and grasslands. *Remote Sens.* **2015**, *7*, 10501–10522. [CrossRef]
88. Quintano, C.; Calvo, L.; Fernández-Manso, A.; Suárez-Seoane, S.; Fernandes, P.M.; Fernández-Guisuraga, J.M. First evaluation of fire severity retrieval from PRISMA hyperspectral data. *Remote Sens. Environ.* **2023**, *295*, 113670. [CrossRef]
89. Miller, J.D.; Thode, A.E. Quantifying burn severity in a heterogeneous landscape with a relative version of the delta Normalized Burn Ratio (dNBR). *Remote Sens. Environ.* **2007**, *109*, 66–80. [CrossRef]
90. Haslem, A.; Leonard, S.W.J.; Bruce, M.J.; Christie, F.; Holland, G.J.; Kelly, L.T.; MacHunter, J.; Bennett, A.F.; Clarke, M.F.; York, A. Do multiple fires interact to affect vegetation structure in temperate eucalypt forests? *Ecol. Appl.* **2016**, *26*, 2414–2423. [CrossRef]
91. R Core Team. *R: A Language and Environment for Statistical Computing*; R Foundation for Statistical Computing: Vienna, Austria, 2021; Available online: https://www.R-project.org/ (accessed on 10 December 2021).
92. Cardil, A.; Mola-Yudego, B.; Blázquez-Casado, Á.; González-Olabarria, J.R. Fire and burn severity assessment: Calibration of Relative Differenced Normalized Burn Ratio (RdNBR) with field data. *J. Environ. Manag.* **2019**, *235*, 342–349. [CrossRef]

93. Meng, R.; Wu, J.; Zhao, F.; Cook, B.D.; Hanavan, R.P.; Serbin, S.P. Measuring short-term post-fire forest recovery across a burn severity gradient in a mixed pine-oak forest using multi-sensor remote sensing techniques. *Remote Sens. Environ.* **2018**, *210*, 282–296. [CrossRef]
94. Miller, J.D.; Quayle, B. Calibration and validation of immediate post-fire satellite-derived data to three severity metrics. *Fire Ecol.* **2015**, *11*, 12–30. [CrossRef]
95. Picotte, J.J.; Cansler, C.C.A.; Kolden, C.A.; Lutz, J.A.; Key, C.; Benson, N.C.; Robertson, K.M. Determination of burn severity models ranging from regional to national scales for the conterminous United States. *Remote Sens. Environ.* **2021**, *263*, 112569. [CrossRef]
96. Fernández-Guisuraga, J.M.; Fernandes, P.M.; Marcos, E.; Beltrán-Marcos, D.; Sarricolea, P.; Farris, M.; Calvo, L. Caution is needed across Mediterranean ecosystems when interpreting wall-to-wall fire severity estimates based on spectral indices. *For. Ecol. Manag.* **2023**, *546*, 121383. [CrossRef]
97. Fernández-García, V.; Quintano, C.; Taboada, A.; Marcos, E.; Calvo, L.; Fernández-Manso, A. Remote Sensing Applied to the Study of Fire Regime Attributes and Their Influence on Post-Fire Greenness Recovery in Pine Ecosystems. *Remote Sens.* **2018**, *10*, 733. [CrossRef]
98. Fernández-Guisuraga, J.M.; Calvo, L.; Quintano, C.; Fernández-Manso, A.; Fernandes, P.M. Fractional vegetation cover ratio estimated from radiative transfer modeling outperforms spectral indices to assess fire severity in several Mediterranean plant communities. *Remote Sens. Environ.* **2023**, *290*, 113542. [CrossRef]
99. Tanase, M.A.; Santoro, M.; De La Riva, J.; Fernando, P.; Le Toan, T. Sensitivity of X-, C-, and L-band SAR backscatter to burn severity in Mediterranean pine forests. *IEEE Trans. Geosci. Remote Sens.* **2010**, *48*, 3663–3675. [CrossRef]
100. Montesano, P.M.; Cook, B.D.; Sun, G.; Simard, M.; Nelson, R.F.; Ranson, K.J.; Zhang, Z.; Luthcke, S. Achieving accuracy requirements for forest biomass mapping: A spaceborne data fusion method for estimating forest biomass and LiDAR sampling error. *Remote Sens. Environ.* **2013**, *130*, 153–170. [CrossRef]
101. Conti, L.; Malavasi, M.; Galland, T.; Komárek, J.; Lagner, O.; Carmona, C.P.; de Bello, F.; Rocchini, D.; Šímová, P. The relationship between species and spectral diversity in grassland communities is mediated by their vertical complexity. *Appl. Veg. Sci.* **2021**, *24*, e12600. [CrossRef]
102. Burgin, M.; Clewley, D.; Lucas, R.M.; Moghaddam, M. A generalized radar backscattering model based on wave theory for multilayer multispecies vegetation. *IEEE Trans. Geosci. Remote. Sens.* **2011**, *49*, 4832–4845. [CrossRef]
103. Kasischke, E.S.; Bourgeau-Chavez, L.L.; Johnstone, J.F. Assessing spatial and temporal variations in surface soil moisture in fire-disturbed black spruce forests in Interior Alaska using spaceborne synthetic aperture radar imagery-Implications for post-fire tree recruitment. *Remote Sens. Environ.* **2007**, *108*, 42–58. [CrossRef]
104. Chen, L.; Ren, C.; Bao, G.; Zhang, B.; Wang, Z.; Liu, M.; Man, W.; Liu, J. Improved Object-Based Estimation of Forest Aboveground Biomass by Integrating LiDAR Data from GEDI and ICESat-2 with Multi-Sensor Images in a Heterogeneous Mountainous Region. *Remote Sens.* **2022**, *14*, 2743. [CrossRef]
105. Broncano, M.J.; Retana, J. Topography and forest composition affecting the variability in fire severity and post-fire regeneration occurring after a large fire in the Mediterranean basin. *Int. J. Wildland Fire* **2004**, *13*, 209–216. [CrossRef]
106. Crecente-Campo, F.; Pommerening, A.; Rodríguez-Soalleiro, R. Impacts of thinning on structure, growth and risk of crown fire in a *Pinus sylvestris* L. plantation in northern Spain. *For. Ecol. Manag.* **2009**, *257*, 1945–1954. [CrossRef]
107. Keeley, J.E. Fire Management of California Shrubland Landscapes. *Environ. Manag.* **2002**, *29*, 395–408. [CrossRef]
108. Paula, S.; Ojeda, F. Resistance of three co-occurring resprouter Erica species to highly frequent disturbance. *Plant Ecol.* **2006**, *183*, 329–336. [CrossRef]
109. Vega, J.A. Empirical approach to fire spread prediction in shrublands. In Proceedings of the Workshop on Mathematical Modeling and Numerical Simulation of Forest Fire Propagation, Vigo, Spain, 29–30 November 2007.
110. Bennett, L.T.; Bruce, M.J.; MacHunter, J.; Kohout, M.; Tanase, M.A.; Aponte, C. Mortality and recruitment of fire-tolerant eucalypts as influenced by wildfire severity and recent prescribed fire. *For. Ecol. Manag.* **2016**, *380*, 107–117. [CrossRef]
111. Bassett, M.; Leonard, S.W.J.; Chia, E.K.; Clarke, M.F.; Bennett, A.F. Interacting effects of fire severity, time since fire and topography on vegetation structure after wildfire. *For. Ecol. Manag.* **2017**, *396*, 26–34. [CrossRef]
112. Bradstock, R.A.; Hammill, K.A.; Collins, L.; Price, O. Effects of weather, fuel and terrain on fire severity in topographically diverse landscapes of south-eastern Australia. *Landsc. Ecol.* **2010**, *25*, 607–619. [CrossRef]
113. Fernández-Guisuraga, J.M.; Fernandes, P.M.; Tárrega, R.; Beltrán-Marcos, D.; Calvo, L. Vegetation recovery drivers at short-term after fire are plant community-dependent in mediterranean burned landscapes. *For. Ecol. Manag.* **2023**, *539*, 121034. [CrossRef]
114. Moreira, B.; Tormo, J.; Pausas, J.G. To resprout or not to resprout: Factors driving intraspecific variability in resprouting. *Oikos* **2012**, *121*, 1577–1584. [CrossRef]
115. Maia, P.; Vasques, A.; Pausas, J.G.; Viegas, D.X.; Keizer, J.J. Fire effects on the seed bank of three Mediterranean shrubs: Implications for fire management. *Plant Ecol.* **2016**, *217*, 1235–1246. [CrossRef]
116. Strydom, T.; Kraaij, T.; Difford, M.; Cowling, R.M. Fire severity effects on resprouting of subtropical dune thicket of the Cape Floristic Region. *PeerJ* **2020**, *8*, e9240. [CrossRef]
117. Keeley, J.E.; Fotheringham, C.J.; Baer-Keeley, M. Determinants of postfire recovery and succession in Mediterranean-climate shrublands of California. *Ecol. Appl.* **2005**, *15*, 1515–1534. [CrossRef]

118. Schwilk, D.W.; Gaetani, M.S.; Poulos, H.M. Oak Bark Allometry and Fire Survival Strategies in the Chihuahuan Desert Sky Islands, Texas, USA. *PLoS ONE* **2013**, *8*, e79285. [CrossRef]
119. Minor, J.; Falk, D.A.; Barron-Gafford, G.A. Fire Severity and Regeneration Strategy Influence Shrub Patch Size and Structure Following Disturbance. *Forests* **2017**, *8*, 221. [CrossRef]
120. Vacchiano, G.; Lonati, M.; Berretti, R.; Motta, R. Drivers of *Pinus sylvestris* L. regeneration following small, high-severity fire in a dry, inner-alpine valley. *Plant Biosyst.* **2015**, *149*, 354–363. [CrossRef]
121. Dzwonko, Z.; Loster, S.; Gawroński, S. Effects of fire severity on understory community regeneration and early succession after burning of moist pine forest. *Tuexenia* **2018**, *38*, 197–214.
122. Huerta, S.; Fernández-García, V.; Calvo, L.; Marcos, E. Soil Resistance to Burn Severity in Different Forest Ecosystems in the Framework of a Wildfire. *Forests* **2020**, *11*, 773. [CrossRef]
123. Calvo, L.; Santalla, S.; Marcos, E.; Valbuena, L.; Tárrega, R.; Luis, E. Regeneration after wildfire in communities dominated by *Pinus pinaster*, an obligate seeder, and in others dominated by *Quercus pyrenaica*, a typical resprouter. *For. Ecol. Manag.* **2003**, *184*, 209–223. [CrossRef]
124. Pausas, J.G.; Keeley, J.E. Evolutionary ecology of resprouting and seeding in fire-prone ecosystems. *New Phytol.* **2014**, *204*, 55–65. [CrossRef]
125. Broncano, M.J.; Retana, J.; Rodrigo, A. Predicting the Recovery of *Pinus halepensis* and Quercus ilex Forests after a Large Wildfire in Northeastern Spain. *Plant Ecol.* **2005**, *180*, 47–56. [CrossRef]
126. Barbeta, A.; Peñuelas, J. Sequence of plant responses to droughts of different timescales: Lessons from holm oak (*Quercus ilex*) forests. *Plant Ecol. Divers.* **2016**, *9*, 321–338. [CrossRef]
127. Smith, M.G.; Arndt, S.K.; Miller, R.E.; Kasel, S.; Bennett, L.T. Trees use more non-structural carbohydrate reserves during epicormic than basal resprouting. *Tree Physiol.* **2018**, *38*, 1779–1791. [CrossRef]
128. Quintano, C.; Fernández-Manso, A.; Calvo, L.; Roberts, D.A. Vegetation and Soil Fire Damage Analysis Based on Species Distribution Modeling Trained with Multispectral Satellite Data. *Remote Sens.* **2019**, *11*, 1832. [CrossRef]